Int. J. Electrochem. Sci., 10 **(2015)** 10651 - 10658

International Journal of
ELECTROCHEMICAL
SCIENCE
www.electrochemsci.org

Short Communication

Facile Synthesis of High-quality N-doped Graphene Anchored with Fe_2O_3 for Use As Lithium-ion Battery Anode Materials

Chuanning Yang, Yongquan Qing, Yan Shang, Youzheng Sun, Changsheng Liu [*]

Key Laboratory for Anisotropy and Texture of Materials of Ministry of Education, Northeastern University, Shenyang, Liaoning 110004, China
[*]E-mail: ycnsuper@163.com, csliu@mail.neu.edu.cn

Received: 30 September 2015 / *Accepted:* 17 October 2015 / *Published:* 4 November 2015

A hybrid material composed of nitrogen-doped graphene anchored with Fe_2O_3 was readily obtained by a facile and one-step hydrothermal method followed by assisting with microwave under mild conditions. Scanning electron microscopy and transmission electron microscopy images show that Fe_2O_3 with average size of 30-50 nm are homogeneously distributed and anchored on the surface of nitrogen-doped graphene sheets. The N-doped graphene/Fe_2O_3 hybrid electrodes exhibit excellent electrochemical performance with the charge/discharge capacity maintain stable at around 844.3 $mAhg^{-1}$ and 937.7 $mAhg^{-1}$ after the 40 th cycle. The enhanced lithium-storage performance is ascribed to the rational design of the hybrid and has a great potential as anode material for lithium ion batteries.

Keywords: lithium-ion battery; anode materials; graphene; Fe_2O_3

1. INTRODUCTION

For now, rechargeable lithium ion batteries (LIBs) are widely utilized in a range of secondary energy storage devices of portable electronic devices due to their high power density, high safety and long cycle life [1-3]. However, the conventional graphite electrode shows a relatively low specific capacity (372 mAH g^{-1}) calculated by forming the compound of LiC_6 which cannot meet the current demands for high capacity lithium ion batteries [4]. Transition metal oxides (MO) such as Fe_3O_4 [5], SnO_2 [6], Co_3O_4 [7], MoO_2 [8] and NiO [9] with enhanced electrochemical properties have been extensively investigated as anode materials for LIBs. AS one of the most promising anode materials, Fe_2O_3 has received much attention owing to its high theoretical capacity, low cost and plenty [10,11]. However, hindered by a large volume expansion during Li^+ insertion /extraction, Fe_2O_3 shows poor electrochemical property as anode material for LIBs [12,13]. To overcome the drawback caused by mentioned above, graphene is the most promising matrix to anchor nanoparticles and alleviate the

large volume change due to its inherent outstanding properties such as large specific surface area, high electrical conductivity, good flexibility, and high chemical stability [14]. Furthermore, nitrogen-doped grapheme (NGr) is one typical form of chemically-modified graphene compounds which has been aroused the attention attributing to its superior specific capacity for the introduction of nitrogen atoms with numerous outstanding properties such as the increased disorder on the surface, excellent hydrophobicity, improved electrode electrolyte wettability, and enhanced electrochemical activity[15-17].

Herein, we demonstrate a facile and reliable approach to fabricate high-quality N-doped graphene anchored with Fe_2O_3 for lithium ion battery anode with excellent electrochemical performance. Moreover, no toxic materials have been used in the whole process of fabrication. The morphology, structure, electrochemical properties and the first charge discharge capacity of N-doped graphene anchored with Fe_2O_3 were also investigated. It is showed that the nanocomposite can fairly meet the current demand for high capacity and quality as the anode material of LIBs.

2. EXPERIMENT

2.1 Preparation of Material

2.1.1 Preparation of nitrogen doped graphene anchored with Fe_2O_3

All reagents used in the experiment were analytical pure without any further purification. Graphene oxide(GO) was fabricated from natural graphite flake(size≈2 μm) by using a modified Hummers method which has been described detailed in our previous work[18].The nitrogen doped graphene anchored with Fe_2O_3 (N-doped graphene/Fe_2O_3) was synthesized by a facile method and one-step of simultaneous hydrothermal synthesis and assembly procedure. A typical synthesis of the N-doped graphene/Fe_2O_3 hybrids was as follows: 10.8 g urea was added into the 60 ml 2 mg ml^{-1} GO solution by ultrasonication stirring technology for 30 min. Then 6 m mol $FeSO_4 \cdot 6H_2O$ was introduced into the above solution followed by ultrasonication for another 30 min. The whole mixture as the precursor was transferred to a 100 ml polytetrafluoroethylene Teflon-lined stainless steel autoclave, sealed and maintained at 160 ℃ for 16 h. After the reaction completed, the N-doped graphene/Fe_2O_3 collected by centrifugation, filtration, and washed several times with distilled water and anhydrous ethanol followed by vacuum drying for 12 h. Finally, the production was prepared by microwave treating for 2 min using a household microwave oven (700 W, Galanz) to eliminate the oxygen functional groups on the surface of graphene sheets. Fig.1 shows the shcematic procedure for preparation of N-doped graphene/Fe_2O_3 hybrid.

2.1.2 Characterization of samples

The transmission electron microscopy (TEM) and high-resolution TEM (HRTEM) images were obtained by using a JEOL, JEM-2100F, with the acceleration voltage of 200 kV. Preparation of

the testing samples were ultrasonically dispersed in ethanol and deposited onto copper grids covered with a holey carbon film. The morphologies of the samples were investigated by scanning electron microscopy (SEM), JEOL, JSM-7001F, with the acceleration voltage of 15 kV. The X-ray diffraction (XRD) patterns of the synthesized samples were studied by an X'Pert Pro diffractometer (PANalytical Co., Holland) with Cu Kα radiation (40 kV and 40 mA) at room temperature.

2.1.3 Electrochemical measurement

Electrochemical performance of the composite electrodes assembled in a coin cell configuration (CR 2032-type), and were tested in a LAND battery testing system which conducted between 0.01-3 V vs Li^+/Li with the lithium metal foil working as the counter electrode. A slurry coating procedure was utilized to prepare the working electrode which consist of active materials, carbon black and PVDF with a weight ratio of 80:10:10 followed by mixing sufficiently in N-methylpyrrolldinone (NMP), after that the samples coated in the Cu foil and dried under at 80 ℃ overnight in vacuum. Before the whole assembly procedure, all the samples were needed to dry at 75 ℃ for 3 h to remove the residual moisture and impurities.

The 2032 coin cell were assembled in an argon-filled glove box with the electrolyte consisting of 1M LiPF6 dissolved in the solution with 1:1 ethylene carbonate and diethyl carbonate by volume, and the separator (Celgard 2340, USA) was added between the working electrode and the counter electrode. All the electrochmical measurements were carried out at room temperature.

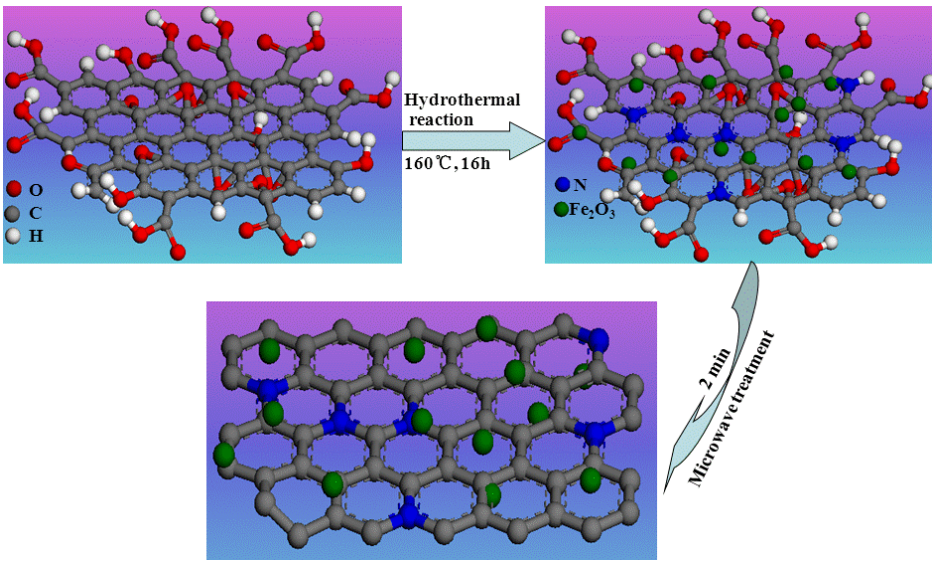

Figure 1. Schematic illustration for the synthesis mechanism of the N-doped graphene/Fe_2O_3.

3. RESULTS AND DISCUSSION

The phase structure of the testing material was characterized by XRD measurement. The XRD pattern of the N-doped graphene/Fe_2O_3 hybrid nanocomposite can be observed in Fig.2. There are two

different Fe_2O_3 crystal structures coexisting in the hybrids which are hematite(α) and maghemite (γ) Fe_2O_3.For the samples, the diffraction peaks appear at 2θ=20.04º, 24.17º, 30.11º, 33.05º, 35.51º, 40.89º, 43.13º, 49.35º, 53.90º, 57.47º, 62.44º and 63.98º corresponding to the (200), (012), (411), (104), (110), (113), (202), (024), (116), (122), (214) and (300) planes of α and γcrystal phase Fe_2O_3, respectively. No excess peaks of impurities were shown in the XRD which indicating that Fe_2O_3 particles are absolutely formed on the surface of the nitrogen doped graphene without blending any impurity matters. Besides, the characteristic diffraction peak at about 2θ=25º of graphene cannot be observed which suggesting no aggregation of nitrogen doped graphene happened during the hydrothermal process. The strong interfacial bonding between Fe_2O_3 nanoparticles and nitrogen doped graphene surface effectively keep the separated structure of nitrogen doped graphene and prevent the aggregation of nitrogen doped graphene [19,20].

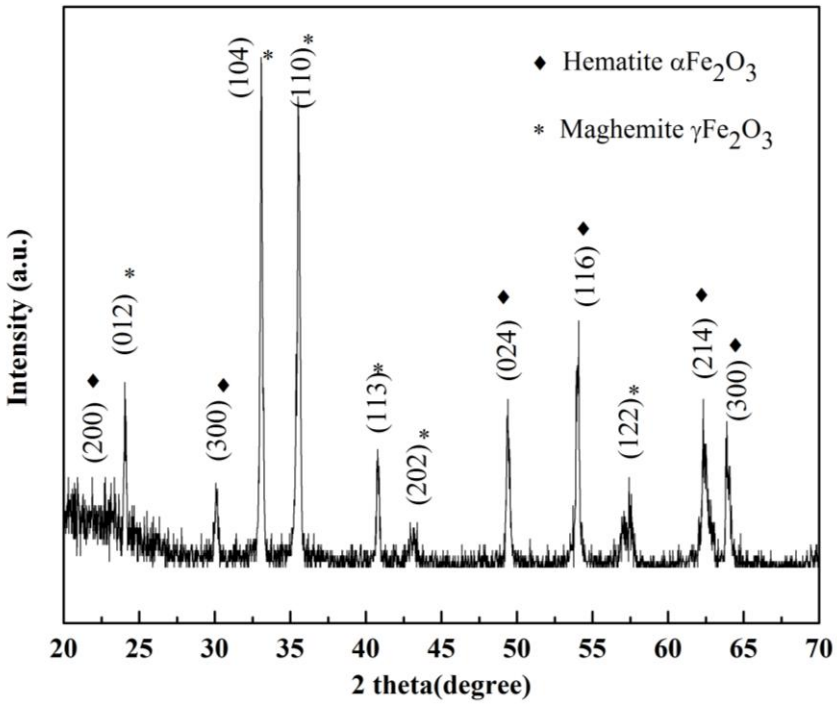

Figure 2. X-ray diffraction (XRD) pattern of the N-doped graphene/Fe_2O_3 with different Fe_2O_3 crystal structures Fe_2O_3.

The surface morphology and structure of the N-doped graphene/Fe_2O_3 were investigated by SEM as shown in Fig.3. It can be clearly observed in the Fig.3(a-c) that a great number of Fe_2O_3 nano-size particles are uniformly and homogeneously distributed on the nitrogen doped graphene sheets which are crumpled to a curly and wavy shape. In addition, the high magnification SEM image (Fig.2(c)) suggests that the nitrogen doped graphene sheets well permeated in Fe_2O_3 nano particles, indicating the successful formation of N-doped graphene/Fe_2O_3 nanocomposite. For further research of the detailed microstructure of the N-doped graphene/Fe_2O_3, the transmission electron microscopy (TEM) images of the N-doped graphene/Fe_2O_3 are clearly revealed in Fig.3(d-f). It can also be obviously observed that the Fe_2O_3 nano particles are about 30-50 nm in size and are homogeneously

distributed on the surface of graphene sheets which are wrinkled transparent flakes. The agglomeration of Fe_2O_3 nano particles with graphene sheets can promote electron transfer during charge/discharge. The NH_3 released from urea boost the formation of pores on the surface of iron oxides during a long hydrothermal process. The HR-TEM image (Fig. 3f) shows the Fe_2O_3 nano particles were surrounded by curly graphene sheets. The lattice fringe spacing of the 0.252 and 0.208 nm correspond in sequence to the inter planar spacing between (110) and (202) planes of α and γFe_2O_3, respectively, which is identical to the previous XRD curve.

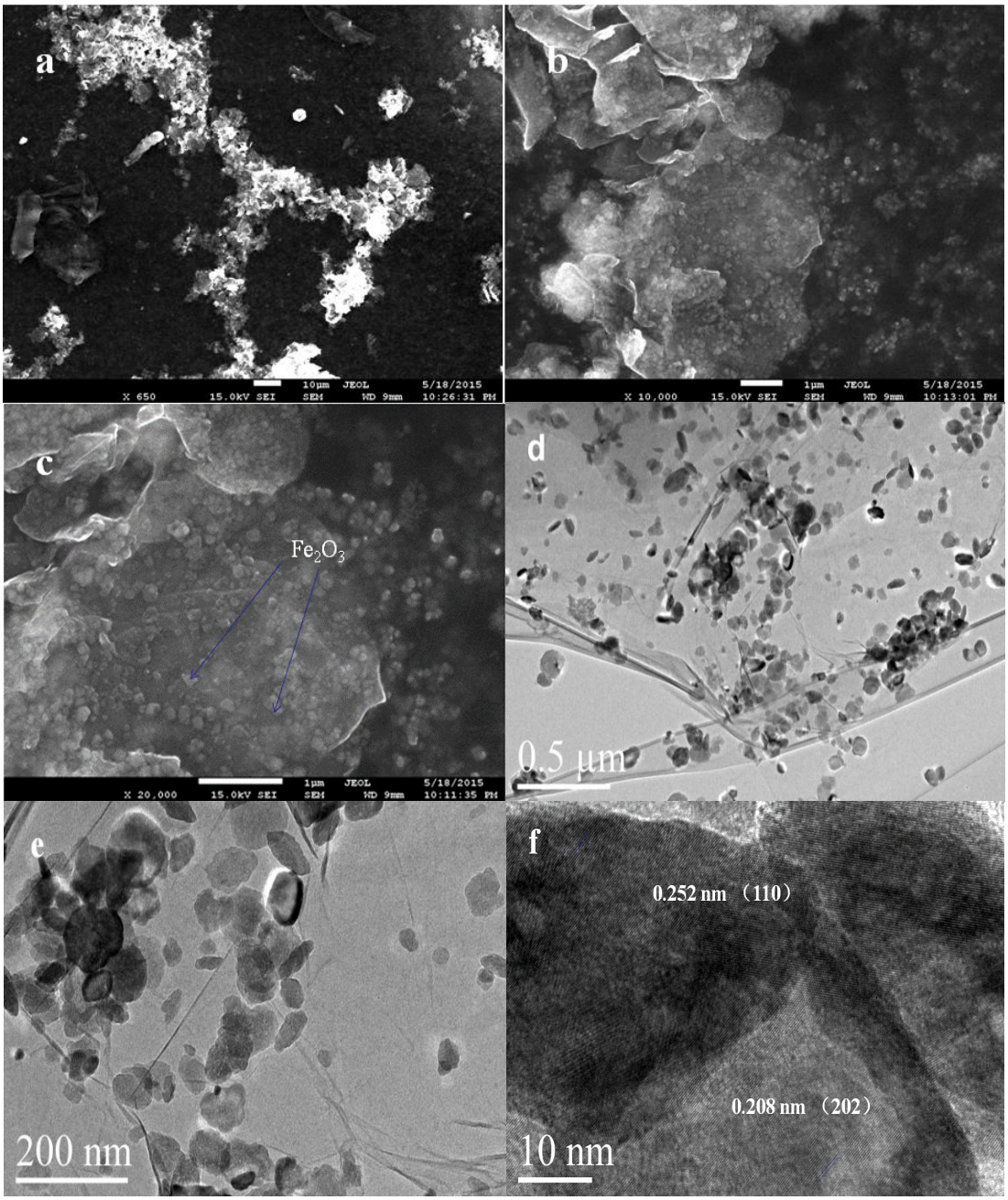

Figure 3. Microstructure and morphology of the N-doped graphene/Fe_2O_3 hybrid electrodes. SEM(a-c) and TEM(d-f) images of the N-doped graphene/Fe_2O_3 composite.

The charge-discharge profiles of the N-doped graphene/Fe_2O_3 hybrid electrodes for the 1st, 2 nd, 10 th and 50 th cycles at a current density of 100 mAg^{-1} were shown in Fig.4. Two obvious plateaus can be observed in the first discharge profiles. The discharge capacities of the hybrid in the 1 st, 2 nd, 10 th and 50 th cycle are 742.6, 678.6, 704.5, 937.7 $mAhg^{-1}$, respectively. The charge capacities of the hybrid in the 2 nd, 10 th and 50 th cycle are 555.9, 610.7 and 844.3 $mAhg^{-1}$, respectively. It is no doubt that the whole cycles have a relatively high Coulombic efficiency except the first cycle which suffered a great capacity loss owing to the formation of solid electrolyte interface (SEI) layer [4,21-23]. It is suggesting that the hybrids electrodes own high electrochemical reversibility as anode materials for lithium ion batteries. The cyclic properties of the N-doped graphene/Fe_2O_3 hybrid electrodes at current density of 100 mAg^{-1} are revealed at Fig.5. The initial discharge/charge capacity of the N-doped graphene/Fe_2O_3 hybrid electrodes is 742.6 $mAhg^{-1}$ and 555.9 $mAhg^{-1}$, respectively, at the current density of 100 mAg^{-1}. The irreversible loss of capacity in the first cycle may be attributed to the formation of SEI layer. After that cycle, the charge and discharge capacity gradually raise from 555.9, 678.6 $mAhg^{-1}$ to 843.8 and 936.7 $mAhg^{-1}$, respectively, in the 40 th cycle. It is generally considered as the activation process of the material [24]. Then the charge/discharge capacity maintain stable at around 844.3 $mAhg^{-1}$ and 937.7 $mAhg^{-1}$ after the 40 th cycle. This phenomenon may be due to the N-doped graphene/Fe2O3 composite lose its crystallinity transform to an amorphous structure, thus enhancing the Li+ diffusion kinetics so that more Li+ can insert into or extract from the material. This excellent capacities might be due to the unique structure of hybrid and the microwave treatment which enhancing the conductivity of hybrid anode by removing the excess oxygen functional groups of graphene sheets.

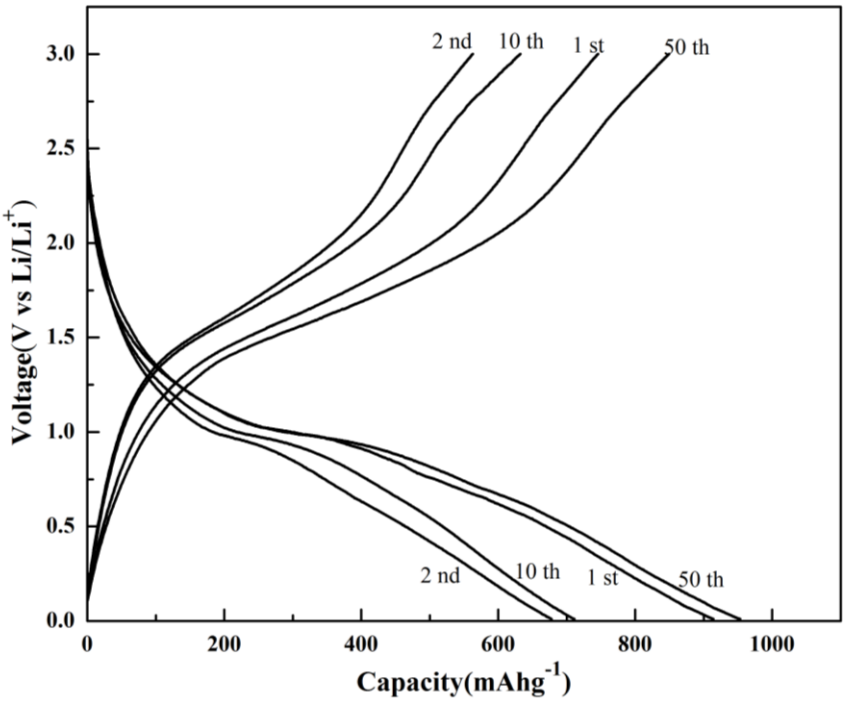

Figure 4. Charge/discharge profiles of the N-doped graphene/Fe_2O_3 hybrid electrodes for the 1st, 2 nd, 10 th and 50 th cycles at a current density of 100 mAg^{-1}.

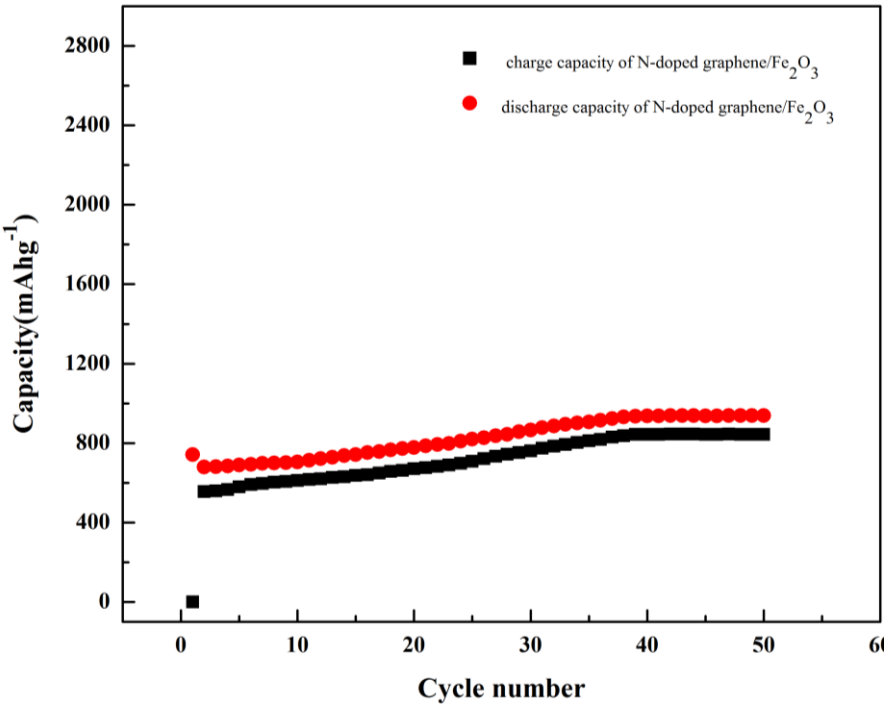

Figure 5. Cyclic performance of the N-doped graphene/Fe_2O_3 hybrid electrodes in the voltage range of 0.01 and 3.0 V at current density of 100 mAg^{-1}.

4. CONCLUSIONS

In summary, a facile and one-step fabrication method was invited to fabricate a nitrogen-doped graphene and Fe_2O_3 with a average size 30-50 nm, were homogeneously distributed and anchored on the surface of nitrogen-doped graphene sheets. The obtained N-doped graphene/Fe_2O_3 hybrid shows excellent nanostructure morphology and electrochemical properties as the anode material for lithium ion batteries. This is due to the unique architecture of the hybrid in which graphene can be treated as the buffer that not only avoid the Fe_2O_3 nanoparticles aggregating on the surface of the nitrogen-doped graphene but also ease the severe volume change during the charge/discharge process. The enhanced lithium-storage performance is ascribed to the rational design of the hybrid and has a great potential as anode material for LIBs.

ACKNOWLEDGEMENTS
The authors gratefully acknowledge financial support from the Ministry of Education Basic Scientific Research Expenses (Grant no. N130810001) and National High Technology Program (863 Project) (Grant no. 2009AA03Z529)

References

1. J. Tarascon and M. Armand, *Nature*, 414 (2001) 359
2. K. Kang, Y. S. Meng, J. Breger, C. L. Grey and G. Ceder, *Science*, 311 (2006) 977

3. C. J. Kuei, W. Chihming and S. Iwen, *J Mater Chem*, 20 (2010) 3729
4. Q. W. Tang, Z. Q. Shan, L. Wang and X. Qin, *Electrochim Acta*, 79 (2012) 148
5. G. M. Zhou, D. W. Wang and F. Li, *Chem Mater*, 22 (2010) 5306
6. M. Armand and J. Tarascon,*Nature*, 451 (2008) 652
7. B. J. Li, H. Q. Cao, J. Shan, G. Q. Li, M. Z. Qu and G. Yin, *Chem*, 50 (2011) 1628
8. V. Srinivasan and J. W. Weidner, *J Electrochem*. Soc, 144 (1997) L220
9. D. Qiu, Z. Xu, M. Zheng, B. Zhao, L. Pan, L. Pu and Y. Shi, *Solid State Electrochem*, 16 (2012) 1889
10. J. Chen, L. Xu, W. Li and X. Gou, *Adv Mater*, 17 (2005) 582
11. G. Zhou, D. Wang, P. Hou, W. Li, N. Li and C. Liu, *J Mater Chem*, 22 (2012) 17942
12. J. Chen, T. Zhu, X. Yang, H. Yang and X. Lou, *J Am Chem Soc*, 132 (2010) 13162
13. P. Poizot, S. Laruelle, S. Grugeon, L. Dupont and J. M. Tarascon, *Nature*, 407 (2000) 496
14. W. W. Zhou, C. Y. Ding, X. T. Jia, Y. Tian, Q. T. Guan and G. W. Wen, *Mater Research Bulletin*, 62 (2015) 19
15. T. Hu, M. Xie, J. Zhong, H. T. Sun, X. Sun, S. Scott, S. M. George, C. S. Liu and J. Lian, *Carbon*, 76 (2014) 141
16. Z. Wu, W. Ren, L. Xu, F. Li and H. Cheng, *ACS Nano*, 5 (2011) 5463
17. T. Hu, X. Sun, G. Xin, D. Shao and C. Liu, *Phys Chem Phys*, 16 (2013) 1060
18. G. K. Wang, X. Sun, F. Y. Lu, M. P. Yu, W. L. Jiang, C. S. Liu and J. Lian, *Small*, 8 (2012) 452
19. Z. W. Yang, Y. Z. Wan, G. Y. Xiong, D. Y. Li, Q. P. Li, C. Y. Ma, R. S. Guo and H. G. Luo, *Mater Res Bull*, 61 (2015) 292
20. H. B. Zhang, W. G. Zheng, Q. Yan, Y. Yang, J. W. Wang, Z. H. Lu, G. Y. Ji and Z. Z. Yu, *Polymer*, 51 (2010) 1191
21. M. Itagaki, S. Yotsuda, N. Kobari, K. Watanabe, S. Kinoshita and M. Ue, *Electrochimica Acta*, 51 (2006) 1629
22. S. K. Martha, E. Markevich, V. Burgel, G. Salitra, E. Zinigrad, B. Markovsky, H. Sclar, Z. Pramovich, O. Heik, D. Aurbach, I. Exnar, H. Buqa, T. Drezen, G. Semrau, M. Schmidt, D. Kovacheva and N. Saliyski, *J Power Sources*, 189 (2009) 288
23. J. O. Besenhard, M. Winter, J. Yang and W. Biberacher, *J Power Sources*, 54 (1995) 228
24. Z. Li, Y. Mi, X. Liu, S. Liu, S. Yang and J. Wang, *J Mater Chem*, 21 (2011) 14706